Published in final edited form as:
J Neurosci. 2013 February 27; 33(9): 4165–4180. doi:10.1523/JNEUROSCI.4185-12.2013.

Tbr2 expression in Cajal-Retzius cells and intermediate neuronal progenitors is required for morphogenesis of the dentate gyrus

Rebecca D. Hodge[1,2,*], **Alfredo J. Garcia III**[2], **Gina E. Elsen**[2], **Branden R. Nelson**[1,2], **Kristin E. Mussar**[2], **Steven L. Reiner**[3], **Jan-Marino Ramirez**[1,2], and **Robert F. Hevner**[1,2,*]

[1]Department of Neurological Surgery, University of Washington, Seattle, Washington, United States of America

[2]Center for Integrative Brain Research, Seattle Children's Research Institute, Seattle, Washington, United States of America

[3]Departments of Microbiology, Immunology, and Pediatrics, College of Physicians and, Surgeons, Columbia University, New York, New York, United States of America

Abstract

The dentate gyrus (DG) is a unique cortical region whose protracted development spans the embryonic and early postnatal periods. DG development involves large-scale reorganization of progenitor cell populations, ultimately leading to the establishment of the subgranular zone (SGZ) neurogenic niche. In the developing DG, the T-box transcription factor *Tbr2* is expressed in both Cajal-Retzius cells derived from the cortical hem that guide migration of progenitors and neurons to the DG, and intermediate neuronal progenitors (INPs) born in the dentate neuroepithelium that give rise to granule neurons. Here we show that in mice *Tbr2* is required for proper migration of Cajal-Retzius cells to the DG, and, in the absence of *Tbr2*, formation of the hippocampal fissure is abnormal, leading to aberrant development of the transhilar radial glial scaffold and impaired migration of progenitors and neuroblasts to the developing DG. Furthermore, loss of *Tbr2* results in decreased expression of *Cxcr4* in migrating cells, leading to a premature burst of granule neurogenesis during early embryonic development accompanied by increased cell death in mutant animals. Formation of the transient subpial neurogenic zone was abnormal in *Tbr2* conditional knockouts, and the stem cell population in the DG was depleted prior to proper establishment of the SGZ. These studies indicate that *Tbr2* is explicitly required for morphogenesis of the DG, and participates in multiple aspects of the intricate developmental process of this structure.

Introduction

The dentate gyrus (DG) has a prolonged developmental period that spans embryonic and early postnatal stages and involves large-scale reorganization of progenitor cells (Pleasure et al., 2000; Li and Pleasure, 2005; Li et al., 2009). DG development commences as neural stem cells (NSCs) located in the dentate neuroepithelium (DNe) begin to proliferate (Fig. 1A). NSCs exit the DNe and migrate along the dentate migratory stream (DMS) to form the transient subpial neurogenic zone (SPZ), which organizes around the pole of the developing DG and begins to generate neurons that seed the suprapyramidal blade of the granule cell

[*]Corresponding authors: Rebecca D. Hodge (rdhodge@uw.edu) or Robert F. Hevner, (rhevner@uw.edu). Seattle Children's Research Institute, Center for Integrative Brain, Research, MS C9S-10, 1900 9th Avenue, Seattle, WA, 98101.

Author Contributions:
R.D.H., A.J.G., J.M.R., B.R.N, and R.F.H. designed research. R.D.H., A.J.G., G.E.E., and K.E.M. performed research. R.D.H, A.J.G, and R.F.H analyzed data. S.L.R. contributed unpublished reagents/analytic tools. R.D.H, A.J.G, and R.F.H. wrote the paper.

The authors declare no competing financial interests.

layer (GCL) (Li and Pleasure, 2005; Li et al., 2009). Ultimately, NSCs undergo a second reorganization to establish the subgranular zone (SGZ), the neurogenic niche maintained throughout adulthood (Fig. 1). During postnatal development, NSCs in the SGZ and DMS continue to generate granule neurons that expand both the suprapyramidal and infrapyramidal blades, giving the DG its characteristic arrowhead shape.

Relatively little is known about factors controlling transit of NSCs and neurons to the developing DG. However, Cajal-Retzius cells, which express Reelin, appear to have a special role in orchestrating DG morphogenesis (Forster et al., 2002; Frotscher et al., 2003; Sibbe et al., 2009). Specifically, Reelin is necessary for proper formation of the transhilar radial glial scaffold that guides migration of cells to the developing DG (Forster et al., 2002; Frotscher et al., 2003). Additionally, Reelin has been implicated in controlling exit of progenitor cells from the SPZ (Li et al., 2009), suggesting that it is a critical regulator of multiple aspects of DG development.

Tbr2, a T-box transcription factor (TF), regulates glutamatergic fate specification in a variety of brain regions, including the DG (Hevner et al., 2006; Hodge et al., 2012). Previous work from our laboratory showed that *Tbr2* is specifically expressed in DG intermediate neuronal progenitors (INPs) and established this TF as a critical regulator of neurogenesis in the developing and adult DG (Hodge et al., 2008; Hodge et al., 2012). Here we show that *Tbr2* has additional, novel functions during DG morphogenesis, distinct from its role in regulating neurogenesis. Specifically, we show that *Tbr2* is expressed in Cajal-Retzius cells derived from the cortical hem and that ablation of *Tbr2* in these cells results in ectopic accumulation of Cajal-Retzius cells during their migration to the developing DG. Concurrently, invagination of the pial surface to form the hippocampal fissure is delayed and development of the transhilar radial glial scaffold is aberrant. Moreover, we show that *Tbr2* ablation results in decreased *Cxcr4* expression, suggesting that chemokine signaling is also impaired in the absence of *Tbr2*. Downstream consequences of these defects include accumulation of NSCs in the SPZ in conditional *Tbr2* knockout mice (*Nestin*-Cre;$Tbr2^{flox/flox}$). Subsequently, NSCs fail to localize to the SGZ, leading to a near-complete absence of the adult neurogenic niche. Taken together, these results suggest that *Tbr2* expression is critical for the execution of a series of events that cumulatively orchestrate the complex developmental plan of the DG.

Materials and Methods

Animals

$Tbr2^{flox}$, *Nestin*-Cre, *Nestin*-$CreER^{T2}$, and *Nestin*-GFP mice have been previously described (Tronche et al., 1999; Mignone et al., 2004; Imayoshi et al., 2006; Intlekofer et al., 2008). Animals were maintained on a C57Bl/6 background in the vivarium at Seattle Children's Research Institute (SCRI). Institutional Animal Care and Use Committees at SCRI and the University of Washington approved animal procedures. For experiments using *Nestin*-Cre, control animals were either *Nestin*-Cre;$Tbr2^{flox/+}$ or $Tbr2^{flox/+}$. No differences between these genotypes were observed with respect to brain weight, morphology of the DG, and cell numbers; accordingly, these mice were grouped together as controls (Hodge et al., 2012). Experimental animals were *Nestin*-Cre;$Tbr2^{flox/flox}$. For experiments using the tamoxifen-inducible *Nestin*-$CreER^{T2}$, control animals were *Nestin*-$CreER^{T2}$;$Tbr2^{flox/+}$ and experimental animals were *Nestin*-$CreER^{T2}$;$Tbr2^{flox/flox}$. To generate embryonic mice, timed matings were used with the day of the vaginal plug considered embryonic day (E) 0.5. Embryos were harvested as described (Englund et al., 2005). To collect tissues at postnatal timepoints, animals were deeply anesthetized with Avertin (Sigma) and transcardially perfused with 4% paraformaldehyde (PFA) as described (Hodge et al., 2012). For BrdU

pulse chase experiments, pregnant females were injected with BrdU (50 mg/kg) on E15.5, and embryos were collected on E17.5.

Tamoxifen treatment

Tamoxifen (TAM, Sigma) was dissolved in corn oil (Fisher Scientific) at a concentration of 25 mg/ml. Pregnant females were injected with Tamoxifen (i.p.) on E13.5 and E14.5 at a dosage of 180 mg/kg body weight. Embryos were subsequently collected on E19.5.

Tissue preparation, immunohistochemistry, *in situ* hybridization

Brains of embryonic animals were removed from the skull and placed in 4% PFA for 2–4 hrs, transferred to 30% sucrose and stored at 4°C until they were embedded in OCT (TissueTek). Brains were sectioned at 15–20 μm on a cryostat, mounted on Superfrost Plus glass slides (Fisher Scientific), and stored at −80 °C. Postnatal brains were fixed for 2–4 hrs after perfusion with 4% PFA and were sectioned either at 20 μm on a cryostat as above or at 40 μm free floating. Floating sections were transferred to cryoprotectant solution, as described (Hodge et al., 2008), and stored at −20 °C. Primary antibodies used in the present study were chicken anti-GFP (Abcam, 1:500), rabbit anti-Tbr2 (R.F.H. lab, 1:1000), rat anti-Tbr2 (EB Bioscience 1:250), mouse anti-PCNA (Millipore, 1:1000), rabbit anti-p73 (Santa Cruz, 1:75), rabbit anti-Prox1 (S. Pleasure, 1:500), goat anti-NeuroD1 (Santa Cruz, 1:400), mouse anti-calretinin (Millipore, 1:1000), goat anti-Sox2 (Santa Cruz, 1:400), rabbit anti-Blbp (Abcam, 1:1000), rat anti-Ctip2 (Abcam, 1:500), mouse anti-Reelin (Calbiochem, 1:1000), rabbit anti-Gfap (Dako, 1:1000), and rabbit anti-activated caspase-3 (AC3, Cell Signaling Technologies, 1:500). Sections were processed for the detection of antigens of interest using Alexa Fluor conjugated fluorescent secondary antibodies (Invitrogen) as previously described (Hodge et al., 2008). Nissl stains were performed as described (Hodge et al., 2005). *In situ* hybridization was performed on slide-mounted tissues exactly as previously described (Bedogni et al., 2010). Plasmids to make *in situ* probes for *Cxcl12* and *Cxcr4* were obtained from S. Pleasure (University of California, San Francisco), and *Wnt3a* and *Wnt5a* were from E. Grove (University of Chicago).

Cell counting and surface area measurements

Cell densities (Reelin+, Prox1+, AC3+ cells) were assessed by conducting cell counts on every 10th 20μm section through the rostrocaudal extent of the DG (N=3 animals per group). Images were obtained using a Zeiss LSM 710 confocal microscope equipped with a 40X, 1.3 N.A. oil objective. Cells intersecting the top-plane of focus were excluded from counts, and total cell numbers were divided by the total counting area to give the number of cells per mm^2. To determine the proportion of Sox2+ cells coexpressing Prox1, total numbers of Sox2+, Sox2+/Prox1+, and Prox1+ cells were counted on 3 non-consecutive sections through the DG, and the total number of Sox2+/Prox1+ cells was divided by the total number of Sox2+ cells. For BrdU pulse chase experiments, total numbers of BrdU+ and BrdU+/Prox1+ cells were counted on 3 non-consecutive sections per animal, and the proportion of BrdU+/Prox1+ cells was determined by dividing by the total number of BrdU + cells. The surface area of the hippocampal fissure was measured as previously described (Hodge et al., 2005).

Electrophysiology

Whole cell patch clamp recordings were made from within the GCL of the DG in hippocampal brain slices (400–550μm thick; P15–30). All recordings were conducted in current clamp configuration (sampled at 20kHz) using a multiclamp amplifier and Clampex 10.0 software m (Molecular Devices). Borosilicate glass recording electrodes (4–8MΩ) were prepared using a P-97 Flaming/Brown mircopipette puller (Sutter Instrument Co., Novato,

CA) and filled an with intracellular patch electrode solution containing (in mM) 140 K-gluconic acid, 1 $CaCl_2$, 10 EGTA, 2 $MgCl_2$, 4 Na_2ATP, 10 HEPES (pH=7.2). Upon establishing a stable intracellular recording, a current injection step protocol (−120 to 20pA with a 20pA step) was performed. Measurements were made in triplicate. The mean value of the triplicate measurements was considered as the response of a given neuron during the aforementioned conditions. The calculated junction potential of 12mV was subtracted post-hoc from membrane potential (V_m). Input resistance (R_n) of each neuron was calculated using the changes in V_m that resulted from the hyperpolarizing current injections. The number of action potentials generated by injecting +20pA was also determined.

Statistical Analyses

Statistical analyses were conducted using either ANOVA with Bonferroni *post hoc* analysis or a two-sample t-test where appropriate and as indicated using SPSS statistical software (IBM). Differences were considered statistically significant at $P<0.05$.

Results

Early development of the cortical hem and Dentate Neuroepithelium (DNe) is normal in the absence of *Tbr2*

Previous work from our lab showed that Tbr2 protein is expressed throughout DG development (Hodge et al., 2012); however, the function of *Tbr2* during initial development of the DNe was unclear from these studies. We first examined Tbr2 protein expression on E12.5, and found that Tbr2 was expressed in the cortical hem adjacent to the DNe and in the DNe itself in control animals (Fig. 1G-G1). However, in *Nestin*-Cre;*Tbr2*$^{flox/flox}$ mice, Tbr2 was effectively ablated from the cortical hem and DNe by E12.5 (Fig. 1H-H1). To determine if ablation of *Tbr2* affected development of the cortical hem, we examined several signaling molecules specifically expressed in this region (Fig. 1A, I–L). We found that the cortical hem specific genes *Wnt3a* and *Wnt5a* (Grove et al., 1998; Shimogori et al., 2004) were expressed at levels approximately equivalent to controls in *Nestin*-Cre;*Tbr2*$^{flox/flox}$ mice at E12.5 despite ablation of *Tbr2* in the cortical hem (Fig. 1I–L). As well, early formation of the DNe appeared largely normal (Fig. 1. M-N1) despite the absence of *Tbr2* in mutant mice. In *Nestin*-Cre;*Tbr2*$^{flox/flox}$ mice approximately equal numbers of Nestin-GFP+ NSCs were present in the DNe (Fig. 1M, N). However, we noted that there was an apparent slight reduction in NeuroD1+ and Prox1+ cells in the developing DG in *Nestin*-Cre;*Tbr2*$^{flox/flox}$ animals as compared to control mice at E14.5 (Fig. 1M-N1), consistent with the role of *Tbr2* in DG neurogenesis (Hodge et al., 2012).

Aberrant development of the hippocampal fissure and ectopic accumulation of Reelin+ cells in *Nestin*-Cre;*Tbr2*$^{flox/flox}$ mice

To assess the effect of *Tbr2* conditional deletion on DG morphogenesis, we examined the formation of two morphogenic landmarks, the hippocampal fissure and the transhilar radial glial scaffold (Frotscher et al., 2003; Li et al., 2009; Sibbe et al., 2009). Because Reelin+ Cajal-Retzius cells were previously implicated in orchestrating DG morphogenesis (Forster et al., 2002; Frotscher et al., 2003; Sibbe et al., 2009), we began our analysis with this cell population. As mentioned previously, we observed clear expression of Tbr2 protein in the cortical hem (Fig. 1G-G1; Fig. 2A-A3). Consistent with previous reports (Englund et al., 2005; Gu et al., 2011), we confirmed that Tbr2 protein was expressed in Cajal-Retzius cells in the cortical hem by examining coexpression of Tbr2 and the Cajal-Retzius cell markers p73 and Reelin. At E14.5, the majority of Tbr2+ cells in the cortical hem coexpressed p73 (Fig. 2A-A3) and extensive coexpression of Tbr2 and Reelin was also observed at this age, suggesting that most cortical hem-derived Cajal-Retzius cells express Tbr2 during their

generation (Fig. 2C-C1). These findings suggest that *Tbr2* may have unique functions within Cajal-Retzius cells distinct from its role in INPs (Fig. 2A-A3).

To examine the functions of *Tbr2* in Cajal-Retzius cells, levels of Reelin expression were assessed in the cortical hem of E14.5 control and *Nestin*-Cre;*Tbr2*$^{flox/flox}$ mice. We found that Reelin was expressed at approximately equal levels on a per cell basis in the cortical hem of *Nestin*-Cre;*Tbr2*$^{flox/flox}$ mice and control embryos, suggesting that *Tbr2* is not required for Reelin expression in Cajal-Retzius cells (Fig. 2C-C1, D-D1). However, in *Nestin*-Cre;*Tbr2*$^{flox/flox}$ mice, Tbr2 protein was absent from Cajal-Retzius cells in the cortical hem (Fig. 2B-B3, D-D1) at E14.5, confirming ablation of *Tbr2* in these cells in mutants. Despite this lack of *Tbr2* expression in Cajal-Retzius cells, the density of p73+ and Reelin+ cells in the cortical hem did not appear to differ between *Nestin*-Cre;*Tbr2*$^{flox/flox}$ mutants and control mice at E14.5 (Fig. 2A-A3, B-B3, C-C1, D-D1). Likewise, proliferation of p73+ cells appeared normal in the hem of mutant mice. In fact, the majority of p73+ cells in the cortical hem coexpressed PCNA at E14.5 in both controls (Fig. 2E-E3) and *Nestin*-Cre;*Tbr2*$^{flox/flox}$ mice (Fig. 2F-F3). These results suggest that *Tbr2* is not required for the proliferation and generation of cortical hem-derived Cajal-Retzius cells.

At E15.5, Reelin+ cells began to migrate in control mice concurrent with invagination of the pia, forming the presumptive hippocampal fissure (Fig. 1B; Fig. 3A-A1). Conversely, in *Nestin*-Cre;*Tbr2*$^{flox/flox}$ mice initial invagination of the pial surface was delayed, resulting in a truncated hippocampal fissure, and the developing DG failed to take on its characteristic semicircle shape (Fig. 3B-B1). Consequently, the DG of *Nestin*-Cre;*Tbr2*$^{flox/flox}$ mice appeared to be rotated by approximately 90° in comparison to controls (compare Fig. 3A and 3B) at E15.5. By E16.5, invagination of the pial surface and concurrent migration of Cajal-Retzius cells into the hippocampal fissure was readily identifiable in control mice (Fig. 3D-D2). In controls, the majority of Reelin+ cells were observed in the hippocampal fissure, with a smaller population of these cells localized to the DMS (Fig. 3D1-D2). In *Nestin*-Cre;*Tbr2*$^{flox/flox}$ mice, the cumulative density of Reelin+ cells in the hem, DMS, and DG did not appear to be significantly reduced in comparison to controls at E16.5, but ectopic accumulation of Reelin+ cells was apparent in mutant mice (Fig. 3E-E2). Specifically, a substantial number of Reelin+ Cajal-Retzius cells were observed in the DMS and fewer Reelin+ cells were observed in the hippocampal fissure (Fig. 3E-E2) of *Nestin*-Cre;*Tbr2*$^{flox/flox}$ mice, suggesting impaired migration of these cells to the developing DG in mutant animals. Likewise, the surface area of the hippocampal fissure was significantly reduced in *Nestin*-Cre;*Tbr2*$^{flox/flox}$ mice at E16.5 (Fig. 3C, E2) in comparison to controls (Fig. 3C, D2), and the DG of mutant mice appeared to be abnormally shaped (Fig. 3E, E2). Likely as a result of ectopic accumulation of Reelin+ cells in the DMS, the density of Reelin + cells populating the hippocampal fissure was significantly reduced in *Nestin*-Cre;*Tbr2*$^{flox/flox}$ mice at E16.5 (Control = 1874 ±56 cells/mm^2, *Nestin*- Cre;*Tbr2*$^{flox/flox}$ = 1045 ±72 cells/mm^2; t-test; N=3; $P<0.01$). By P3, very few Reelin+ cells were observed in the DMS of control mice (Fig. 3F-F2), and the greatest concentration of Reelin+ cells was observed in the hippocampal fissure. The surface area of the hippocampal fissure had increased in control mice at P3 in comparison to E16.5 as the result of continued growth of the DG (Fig. 3C, D, F). Decreased invagination of the pial surface persisted in P3 *Nestin*-Cre;*Tbr2*$^{flox/flox}$ mice as evidenced by the continued and significant reduction hippocampal fissure surface area in mutants (Fig. 3C, G, G2). Ectopic Reelin+ cells remained concentrated in the DMS of mutant mice at P3 (Fig. 3G, G1). Whereas the greatest density of Reelin+ cells in P3 control mice was observed in the region of the hippocampal fissure overlying the lateral tip of the suprapyramidal DG blade (Fig. 3F), Reelin+ cells in P3 *Nestin*-Cre;*Tbr2*$^{flox/flox}$ mice were more diffusely dispersed throughout the entirety of the hippocampal fissure (Fig. 3G). As well, ectopic accumulation of Reelin+ cells was observed

at the tip of the developing DG in P3 *Nestin*-Cre;*Tbr2*$^{flox/flox}$ mice (Fig. 3G, G2), further supporting abnormal migration of Cajal-Retzius cells in mutant animals.

Formation of the transhilar glial scaffold is aberrant in *Nestin*-Cre;*Tbr2*$^{flox/flox}$ mice

During the course of early DG development, Blbp+ radial glia migrate from the dentate ventricular zone (VZ) to the fimbriodentate junction (FDJ), a transitional region bridging the fimbria and the developing DG (Fig. 1D; Fig. 4A-A1) (Li et al., 2009). These Blbp+ cells contribute to the formation of the transhilar radial glial scaffold, a structure that guides migrating progenitors and neuroblasts to the developing DG (Fig. 1D, 4A-A1) (Frotscher et al., 2003; Li et al., 2009). Later in DG development, Blbp+ cells migrate across the hilus and, ultimately, take up residence in the hippocampal fissure (Fig. 1D, Fig. 4A1, Fig. 4C-C1) (Li et al., 2009). In E16.5 control mice, Blbp+ radial glia were observed exiting the fimbriodentate junction (FDJ) and migrating through the hilus (Fig. 4A-A1). These cells typically did not coexpress Tbr2 protein (data not shown). Some Blbp+ cells extended radial processes across the hilus in control mice (Fig. 4A1). Concurrent with ectopic accumulation of Reelin+ cells on E16.5, Blbp+ radial glial exiting the dentate ventricular zone (VZ) were delayed in their migration to the hippocampal fissure in *Nestin*-Cre;*Tbr2*$^{flox/flox}$ animals (Fig. 4B-B1). Specifically, in mutant mice, the majority of Blbp+ cells remained in the fimbria and FDJ at E16.5 (Fig. 4B1). By P0, Blbp+ cells were enriched in the hippocampal fissure of control mice, and few remained in the either the fimbria or FDJ (Fig. 4C-C1). In *Nestin*-Cre;*Tbr2*$^{flox/flox}$ mice, many Blbp+ cells remained in the fimbria and FDJ on P0, and few cells were observed migrating through the hilus (Fig. 4D-D1). As a result, the hippocampal fissure was largely devoid of Blbp+ cells in mutant mice at P0 (Fig. 4D-D1). Accordingly, Gfap immunostaining at E18.5 clearly illustrated perturbed transhilar glial scaffold development in *Nestin*-Cre;*Tbr2*$^{flox/flox}$ mice (Fig. 4E–H). In controls, Gfap+ processes were enriched in the hippocampal fissure adjacent to Reelin+ Cajal-Retzius cells, and radially oriented processes were also observed extending through the hilus (Fig. 4E, G). In *Nestin*-Cre;*Tbr2*$^{flox/flox}$ mice, Gfap+ processes were sparse in the reduced hippocampal fissure and the remaining processes were oriented randomly across the hilus, failing to obtain the characteristic radial orientation of the transhilar radial glial scaffold (Fig. 4F, H).

Defects in early DG morphogenesis can be rescued by temporally restricting *Tbr2* ablation

Given that Reelin+ Cajal-Retzius cells are critical orchestrators of early DG morphogenesis, we hypothesized that failure to properly form the hippocampal fissure and transhilar radial glial scaffold occurred predominantly as a result of defects in Cajal-Retzius cell development and migration in *Nestin*-Cre;*Tbr2*$^{flox/flox}$ mice. To test this hypothesis, we crossed an inducible *Nestin*-CreER^{T2} Cre-driver with the *Tbr2*^{flox} conditional allele and treated pregnant females with tamoxifen on E13.5 and E14.5. By doing so, we restricted *Tbr2* conditional deletion to later embryonic stages after the bulk of Cajal-Retzius cells were produced in the cortical hem. Therefore, the majority of early-generated Cajal-Retzius cells should be spared from *Tbr2* knockout in this model. Interestingly, reduced DG granule neuron production was readily apparent in *Nestin*-CreER^{T2};*Tbr2*$^{flox/flox}$ mice by E19.5, as illustrated by decreased numbers of NeuroD1+ cells in mutant animals (Fig. 4I–J), consistent with the role of *Tbr2* in regulating DG neurogenesis (Hodge et al., 2012). Accordingly, the developing DG appeared reduced in size (Fig. 4I–J). However, the length and surface area of the hippocampal fissure appeared to be equivalent to age-matched controls in *Nestin*-CreER^{T2};*Tbr2*$^{flox/flox}$ mice (Fig. 4K–L), suggesting that invagination of the pia occurred as usual when *Tbr2* was ablated at later developmental stages. Strikingly, similar densities of Reelin+ Cajal-Retzius cells populated the hippocampal fissure in both control and *Nestin*-CreER^{T2};*Tbr2*$^{flox/flox}$ mice, and there was no evidence of ectopic accumulation of Reelin+ cells in mutant animals, suggesting that normal migration of Cajal-Retzius cells occurred concurrent with invagination of the pia in *Nestin*-

CreER^{T2};*Tbr2*$^{flox/flox}$ mice (Fig. 4K–L). Accordingly, we observed an enrichment of Gfap+ processes in the hippocampal fissure in both control and *Nestin*-CreER^{T2};*Tbr2*$^{flox/flox}$ mice, and radially oriented Gfap+ processes extending through the hilus were apparent in both groups consistent with normal formation of the transhilar radial glial scaffold (Fig. 4K–L). These results suggest that restricting *Tbr2* knockout to later embryonic development largely abrogated defects in DG morphogenesis, supporting the notion that these effects were principally dependent on proper localization of Reelin+ CR cells to the hippocampal fissure.

Tbr2 ablation results in aberrant neurogenesis during DG development

Previous work from our laboratory established that *Tbr2* expression in INPs was required for granule cell neurogenesis in the developing and adult DG (Hodge et al., 2012). To confirm these results, we examined expression of Tbr2 in the E16.5 DG (Fig. 5A-B4). Similar to what we have reported in the adult DG (Hodge et al., 2008; Hodge et al., 2012), we found that a subset of Tbr2+ cells in the dentate VZ coexpressed the NSC marker Sox2 (Fig. 5A1-A3), suggesting that Tbr2 is expressed during the transition from NSC to INP in the developing DG as it is in the adult DG (Hodge et al., 2012). A small cohort of cells coexpressing Sox2 and Tbr2 was also apparent in the DMS, consistent with extensive migration of NSCs and INPs to the developing DG (Fig. 5B1-B4). Unlike Tbr2 and Sox2, Prox1+ cells were largely confined to the developing DG, although scattered Prox1+ cells were observed in the DMS at E16.5 (Fig. 5A, B1-B4). Coexpression of Sox2 and Prox1 was extremely rare at E16.5 (Fig. 5B1-B4). Tbr2+/Prox1+ cells were observed in the DMS (Fig. 5B1-B4). However, these Tbr2+/Prox1+ cells were rare. The majority of Tbr2+ cells in the DMS/DG at E16.5 were Prox1-negative. Likewise, most Prox1+ cells did not coexpress Tbr2 under normal circumstances (Fig. 5B1-B4).

To determine if *Tbr2* was required for granule neurogenesis in the developing DG, we examined the expression of several granule neuron markers on E16.5 (Fig. 5C–F). At this age, new granule neuroblasts, marked by their expression of the transcription factors NeuroD1 and Prox1 (Liu et al., 2000; Pleasure et al., 2000; Schwab et al., 2000; Lavado and Oliver, 2007), were present predominantly in the forming upper blade of the DG in controls (Fig. 5A, C, E), although NeuroD1+ cells were also present in the developing hippocampal CA fields consistent with expression of *NeuroD1* in this lineage (Pleasure et al., 2000). Interestingly, previous work suggested that granule cell generation is drastically reduced following *Tbr2* ablation in spite of increased proliferation of Sox2+ NSCs (Hodge et al., 2012). However, when we examined very early stages of DG development in *Nestin*-Cre;*Tbr2*$^{flox/flox}$ mice, we found that increased numbers of NeuroD1+/Prox1+ neuroblasts were present along the extent of the DMS in mutants (Fig. 5D–F), in contrast to the decrease in NeuroD1+ neuroblasts we observed when later stages of DG development (P3) were examined in *Nestin*-Cre;*Tbr2*$^{flox/flox}$ animals (Fig. 5P) (Hodge et al., 2012). As well, the DMS appeared to be expanded in *Nestin*-Cre;*Tbr2*$^{flox/flox}$ mice, and both NeuroD1+ and Prox1+ cells were widely dispersed throughout the enlarged DMS in mutants (Fig. 5D, F), well outside of the compartments they were confined to in age-matched controls (Fig. 5C, E). Quantification of Prox1+ neuroblasts at E16.5 revealed a significant increase in Prox1+ cells/mm^2 in mutants (Control = 753 ±167 cells/mm^2, *Nestin*-Cre;*Tbr2*$^{flox/flox}$ = 2750 ±349 cells/mm^2; 266% increase; t-test; $P<0.01$). Increased neurogenesis was confirmed in *Nestin*-Cre;*Tbr2*$^{flox/flox}$ mice using a BrdU pulse-chase experiment where BrdU was administered on E15.5 and embryos were collected on E17.5 (Fig. 5K-L1). Relatively few (9.24 ±0.29%) BrdU+ cells colabeled with Prox1 in control embryos (Fig. 5K-K1). However, this number increased significantly in *Nestin*-Cre;*Tbr2*$^{flox/flox}$ animals to 43.15 ±5.65% of total BrdU+ cells (t-test; $P<0.05$; N=2; Fig. 5L-L1, arrows), suggesting that more Prox1+ neuroblasts were generated in *Nestin*-Cre;*Tbr2*$^{flox/flox}$ mice than in controls between E15.5 and E17.5.

To characterize these early-generated neuroblasts further, we examined expression of several NSC markers in these cells, as we had previously shown that these markers were also upregulated in *Nestin*-Cre;*Tbr2*$^{flox/flox}$ mice at E16.5 (Hodge et al., 2012). Interestingly, we found that the proportion of Prox1+ cells that were proliferating in the DMS and DG appeared to be increased in *Nestin*-Cre;*Tbr2*$^{flox/flox}$ mice at E16.5 (Fig. 5G-H3). In E16.5 controls, very few Prox1+ cells coexpressed PCNA (Fig. 5G-G3), whereas Prox1+/PCNA+ cells were readily apparent in the DMS in *Nestin*-Cre;*Tbr2*$^{flox/flox}$ animals (Fig. 5H-H3). As well, many Prox1+ neuroblasts aberrantly expressed markers of NSCs, including Sox2 and Nestin-GFP (Fig. 5I-J3) in *Nestin*-Cre;*Tbr2*$^{flox/flox}$ mice. Increased numbers of Sox2+/Prox1+ cells were observed throughout the DMS and in the developing DG of mutant mice (Fig. 5J-J3). In *Nestin*-Cre;*Tbr2*$^{flox/flox}$ animals, these Sox2+/Prox1+ cells appeared to express low levels of Prox1 (Fig. 5I), as did Prox1+/PCNA+ cells (Fig. 5H2). Quantification of the proportion of total Sox2+ cells coexpressing Prox1 revealed a significant increase in coexpression of these TFs in *Nestin*-Cre;*Tbr2*$^{flox/flox}$ mice (48.8±1.0%, P<0.01; t-test; N=3) compared to controls (11.3±7.2%). In contrast, in control animals Prox1 was typically expressed in granule neuroblasts that were predominantly Nestin-GFP−/Sox2−, and Prox1 and Sox2 were very rarely expressed in the same cells in control embryos (Fig. 5I-I3).

Given that newborn Prox1+ neuroblasts aberrantly coexpressed NSC markers in *Nestin*-Cre;*Tbr2*$^{flox/flox}$ mice, we postulated that this might lead to increased cell death in mutants. Accordingly, there was a marked increase in cell death in the DMS and DG of mutants on E17.5 as revealed by immunostaining for Activated Caspase-3 (AC3) (Fig. 5M–N). Quantification of AC3+ cells revealed a significant increase in *Nestin*-Cre;*Tbr2*$^{flox/flox}$ mice (83.8 ±2.1 cells/mm^2) as compared to controls (34.02 ±3.2 cells/mm^2; t-test; P<0.001; N=3) confirming that many of these early-generated neuroblasts indeed did not survive. Accordingly, by P3, the number of NeuroD1+ neuroblasts was reduced in *Nestin*-Cre;*Tbr2*$^{flox/flox}$ mice with scattered and misplaced NeuroD1+ cells present in a reduced suprapyramidal DG blade and hilus (Fig. 5O–P). Importantly, increased generation of Prox1+ neuroblasts appeared to be transient in *Nestin*-Cre;*Tbr2*$^{flox/flox}$ mice and was restricted to E15.5 to E17.5. After this time, a reduction in NeuroD1+ and Prox1+ neuroblasts was observed in mutants, similar to our previous report (Hodge et al., 2012). Additionally, we did not observe any increase in NeuroD1+ neuroblasts in *Nestin*-CreER^{T2};*Tbr2*$^{flox/flox}$ mice in which tamoxifen was given to knockout *Tbr2* between E13.5–E14.5 (Fig. 4I–J). Therefore, the transient increase in neuroblasts seen in *Nestin*-Cre;*Tbr2*$^{flox/flox}$ animals appeared to result from the specific environmental circumstances in which the DG developed in these particular mutants.

Interestingly, the premature neurogenesis observed in *Nestin*-Cre;*Tbr2*$^{flox/flox}$ mice between E15.5–E17.5 resembled that previously reported in *Cxcr4* knockout animals (Li et al., 2009). To determine if alteations in this chemokine signaling pathway may account in part for the burst of premature neuroblast generation seen in *Nestin*-Cre;*Tbr2*$^{flox/flox}$ animals, we examined expression of the *Cxcr4* receptor and one of its ligands, *Cxcl12,* in control and mutant animals at several different stages of DG development (Fig. 6). We found that while *Cxcl12* seemed to be expressed at approximately normal levels on a per cell basis, it appeared that overall expression in the hippocampal fissure was slightly reduced in *Nestin*-Cre;*Tbr2*$^{flox/flox}$ mice at both E16.5 and P0 (Fig. 6A–D), likely owing to the decreased number of Cajal-Retzius cells populating the hippocampal fissure and reduced invagination of the pia in mutant animals, as discussed previously. In contrast, expression of *Cxcr4* was markedly decreased in the DMS and DG of *Nestin*-Cre;*Tbr2*$^{flox/flox}$ mice, consistent with the known expression of this receptor in migrating progenitors and neuroblasts (Berger et al., 2007), at both E16.5 and P0 (Fig. 6E–H). These findings suggest that perturbed chemokine signaling may contribute to aberrant migration and premature neurogenesis in

Nestin-Cre;*Tbr2*$^{flox/flox}$ mice, similar to what has been reported in *Cxcr4* knockout animals (Li et al., 2009).

Development of the SPZ and transition to the SGZ are disrupted in *Nestin*- Cre;*Tbr2*$^{flox/flox}$ mice

The SPZ is a transient neurogenic niche that forms around the pole of the developing DG during late stages of embryonic development (Li et al., 2009). Previous studies showed that the SPZ is present until approximately P3-P4, at which time some of the progenitor cells remaining in this zone transition through the GCL and contribute to the formation of the SGZ (Li et al., 2009). To determine if conditional *Tbr2* ablation impacted the development of the SPZ niche, we examined the migration of Nestin-GFP+/Sox2+ NSCs and INPs to the SPZ in *Nestin*-Cre;*Tbr2*$^{flox/flox}$ and control mice at several stages of development (Fig. 7). In control mice, the SPZ was apparent by E16.5 as Nestin-GFP+ NSCs began to concentrate above the forming suprapyramidal DG blade adjacent to the molecular layer (ML) (Fig. 7A-A1). In contrast, Nestin-GFP+ precursors failed to reach SPZ on E16.5 in *Nestin*-Cre;*Tbr2*$^{flox/flox}$ mice and were instead concentrated in the expanded DMS, consistent with aberrant expression of NSC markers in prematurely generated neuroblasts in mutant mice (Fig. 7B-B1). By P0, the SPZ was well formed in control mice, as Nestin-GFP+ NSCs were concentrated above Prox1+ neuroblasts in the forming upper blade of the DG (Fig. 7C-C1 arrows). Many Nestin-GFP+ cells in the SPZ were Sox2+ in P0 control mice (Fig. 7C1). Despite the delay we observed in SPZ formation in *Nestin*-Cre;*Tbr2*$^{flox/flox}$ mice at E16.5, this niche was apparent by P0 in mutants, and, interestingly, increased numbers of Nestin-GFP+/Sox2+ NSCs were observed in the SPZ in these mice (Fig. 7D-D1).

By P3, translocation of Nestin-GFP+ NSCs through the upper GCL out of the SPZ had begun in control mice (Fig. 7E-E1). At this time, Nestin-GFP+ cells became increasingly concentrated in the hilus and forming SGZ in controls, as the generation of the lower (infrapyramidal) DG blade began (Fig. 7E-E1). Conversely, Nestin-GFP+ cells remained concentrated in the SPZ of *Nestin*-Cre;*Tbr2*$^{flox/flox}$ mice at P3 (Fig. 7F-F1 arrows). By P4, the SPZ was largely depleted in control mice and the majority of Nestin-GFP+ NSCs were concentrated in the SGZ of the suprapyramidal blade and in the forming end of the lower blade (Fig. 7G-G1). In contrast, a large number of Nestin-GFP+ NSCs remained in the SPZ of *Nestin*-Cre;*Tbr2*$^{flox/flox}$ mice at P4 (Fig. 7H-H1 arrows) and were somewhat removed from the reduced suprapyramidal DG blade due to expansion of the SPZ. Scattered Nestin-GFP+ progenitors were also observed in the SGZ in *Nestin*-Cre;*Tbr2*$^{flox/flox}$ mice and in the hilus and adjacent tip of the forming infrapyramidal blade (Fig. 7H). However, very few Prox1+ cells were seen in the lower blade in *Nestin*-Cre;*Tbr2*$^{flox/flox}$ mice at P4 (Fig. 7H1), in contrast with controls where new neuroblasts were beginning to expand the lower blade (Fig. 7G1). By P7, translocation of Nestin-GFP+ progenitors out of the SPZ was essentially complete in control mice and the SGZ was readily identifiable, particularly in the upper GCL (Fig. 7I, arrows), although scattered Nestin-GFP+ progenitors could still be seen migrating through the GCL. In P7 *Nestin*-Cre;*Tbr2*$^{flox/flox}$ mice, Nestin-GFP+ NSCs persisted in the SPZ, as they did in earlier stages of development, and few of these NSCs were present in the SGZ of the suprapyramidal GCL (Fig. 7J). Strikingly, granule neurons were largely absent from the infrapyramidal blade in *Nestin*-Cre;*Tbr2*$^{flox/flox}$ mice at P7; instead, this region was populated by Nestin-GFP+ NSCs (Fig. 7J). The suprapyramidal blade of the DG was also obviously reduced in size by P7 in mutant mice (Fig. 7J). In control mice, the SGZ was clearly formed by P14, and the majority of remaining Nestin-GFP+ NSCs had localized to this zone by this time (Fig. 7K). In contrast, the SGZ of *Nestin*-Cre;*Tbr2*$^{flox/flox}$ mice was greatly reduced, consisting only of scattered Nestin-GFP+ NSCs (Fig. 7L). These results suggest that a lasting DG neurogenic niche was essentially

absent from mutant mice (Fig. 7L), consistent with previous reports of *Tbr2* conditional mutant mice (Arnold et al., 2008).

Consequences of loss of *Tbr2* for DG development and function

By the end of DG development (P25; Fig. 8A–B) the DG was greatly reduced in *Nestin*-Cre;*Tbr2*$^{flox/flox}$ mice. The infrapyramidal blade largely failed to form in mutant mice, and the suprapyramidal blade was truncated and significantly thinner in *Nestin*-Cre;*Tbr2*$^{flox/flox}$ mice (Fig. 8A–B). Accordingly, the mossy fiber pathway (the main output of the DG to the hippocampal CA3 field) was markedly reduced in *Nestin*-Cre;*Tbr2*$^{flox/flox}$ mice, as illustrated by reduced Calbindin immunostaining of these axonal projections at P14 (Fig. 8C–D). However, despite ablation of *Tbr2* early in DG development, some Prox1+/Calbindin+ granule neurons were generated in *Nestin*-Cre;*Tbr2*$^{flox/flox}$ mice (Fig. 8E–F). These results suggest that either some NSCs escape *Nestin*-Cre mediated deletion of *Tbr2* and go on to produce granule neurons in *Nestin*-Cre;*Tbr2*$^{flox/flox}$ mice, or that a small population of NSCs/INPs do not require *Tbr2* to produce granule neurons and generate the cells populating the infrapyramidal blade in *Nestin*-Cre;*Tbr2*$^{flox/flox}$ mice.

Given the apparent reduction in mossy fibers and truncation of the DG, we next wanted to test for electrophysiological abnormalities in granule neurons of *Nestin*-Cre;*Tbr2*$^{flox/flox}$ mice and control mice (Fig. 8G). To do so, whole cell patch clamp recordings were made in representative DG granule neurons of both *Nestin*-Cre;*Tbr2*$^{flox/flox}$ (n=9) and control (n=6) hippocampal slices (Fig. 8G). These recordings indicated no significant differences in steady- state V_m (membrane potential) between groups (81 ± 2mV *Nestin*-Cre;*Tbr2*$^{flox/flox}$ vs. 79 ± 3mV control). Interestingly, in 33% of granule neurons recorded in *Nestin*-Cre;*Tbr2*$^{flox/flox}$ mice, injection of +20pA of current evoked action potentials compared to only 14% of control granule neurons. However, R_n (input resistance) in *Nestin*-Cre;*Tbr2*$^{flox/flox}$ granule neurons was significantly smaller (218 ± 16 MΩ) than R_n in control granule neurons (280 ± 24 MΩ; t- test; $P<0.05$) (Fig. 8G). Therefore, while no differences between *Nestin*-Cre;*Tbr2*$^{flox/flox}$ and control neurons were observed with respect to steady-state V_m, a larger percentage of mutant neurons exhibited evoked action potentials. Furthermore, as R_n is a reflection of cell geometry and size as well as the density of ion channels open at resting, the significantly smaller R_n of *Nestin*-Cre;*Tbr2*$^{flox/flox}$ granule neurons suggests that these cells are potentially different both functionally and anatomically from control neurons. Previous reports indicate that R_n varies with the stage of maturity and anatomical position of given DG neurons (Toni et al., 2008; Mongiat et al., 2009). Hence, the observed differences in R_n suggest that the spared DG neurons in *Nestin*-Cre;*Tbr2*$^{flox/flox}$ mice are not fully integrated into the local circuitry, express a different compliment/proportion of intrinsically active channel conductances, and/or are smaller.

Discussion

In the present study, we identify novel functions of *Tbr2* in Cajal-Retzius cells and INPs during morphogenesis of the DG, affirming the importance of this transcription factor in regulating many aspects of DG development (Fig. 9). While a previous study showed that conditional ablation of *Tbr2* during embryonic development (*Sox1*-Cre) impacted DG formation, producing a similar phenotype to the one we have described (Arnold et al., 2008), abnormalities in DG development in this previous study were largely attributed to increased postnatal cell death. We also find increased cell death in our *Nestin*-Cre;*Tbr2*$^{flox/flox}$ model, but we propose this is a downstream outcome of loss of *Tbr2* function that does not fully account for the complex phenotype we observe. Rather, we show that ablation of *Tbr2* in several different cell types impacts multiple steps in DG development that cumulatively result in abnormal morphogenesis, decreased granule neuron production, and altered granule neuron function (Fig. 9).

Previous work from our lab and others showed that *Tbr2* is expressed specifically in INPs from the start of DG development through to adulthood and established a critical role for *Tbr2* in regulating granule cell neurogenesis (Hodge et al., 2008; Roybon et al., 2009; Hodge et al., 2012). Here we show that *Tbr2* is expressed not only in DG INPs but also in the lineage of progenitor cells giving rise to cortical hem-derived Cajal-Retzius cells, and we demonstrate that *Tbr2* has functions within these cells distinct from its role in INPs. Specifically, we show that *Tbr2* is required for proper migration of Cajal-Retzius cells from their place of birth in the cortical hem to the hippocampal fissure during early establishment of the DG (Fig. 9). Our results indicate that aberrant migration of Cajal-Retzius cells to the developing DG may have several downstream consequences for morphogenesis of the GCL that might account for much of the phenotype we observe in *Nestin*-Cre;*Tbr2*$^{flox/flox}$ mice. The first of these defects is impaired development of the transhilar radial glial scaffold (Fig. 9). The importance of Cajal-Retzius cells in establishing this scaffold was first described in *reeler* mice, which are deficient in Reelin expression and lack radially oriented Gfap+ processes consistent with aberrations in the radial glial scaffold (Frotscher et al., 2003; Weiss et al., 2003). Indeed, the DG of *Nestin*-Cre;*Tbr2*$^{flox/flox}$ mice bears some resemblance to that of *reeler* mice, including decreased pial invagination of the hippocampal fissure during early DG morphogenesis (Forster et al., 2002; Weiss et al., 2003). Likewise, *scrambler* mice, which are deficient in Dab1, an intracellular adaptor protein that acts downstream of Reelin, exhibit similar defects in the transhilar radial glial scaffold, further emphasizing the importance of Reelin in orchestrating early DG morphogenesis (Weiss et al., 2003). We show that when *Tbr2* is ablated after the birth of Cajal-Retzius cells in tamoxifen induced *Nestin*-CreER^{T2};*Tbr2*$^{flox/flox}$ mice, Reelin+ cells develop and migrate to the hippocampal fissure, and, in turn, the transhilar glial scaffold develops normally. Thus, abnormalities in DG morphogenesis are largely abrogated when Cajal-Retzius cells develop and migrate on schedule, and *Tbr2* is a critical regulator of Cajal- Retzius cell development. Granule cell neurogenesis, on the other hand, remains impaired in *Nestin*-CreER^{T2};*Tbr2*$^{flox/flox}$ mice, consistent with the known role of *Tbr2* in regulating granule neuron differentiation (Hodge et al., 2012). These results highlight the distinct roles of *Tbr2* in Cajal-Retzius progenitors and granule neuron progenitors (INPs), and emphasize the fact that *Tbr2* must be expressed in both of these populations in order for the DG to develop properly.

Aberrations in the transhilar radial glial scaffold in *Nestin*-Cre;*Tbr2*$^{flox/flox}$ mice likely initiate a cascade of events that lead to further impairments of DG development, including delayed transit of progenitor cells to the forming SPZ. Given that the glial scaffold is thought to act as a guide for migrating cells (Forster et al., 2002; Frotscher et al., 2003; Li et al., 2009), it is possible that physical defects in this scaffold (i.e. lack of radial process orientation) delay migration of progenitors to the forming SPZ. It is likewise possible that changes in expression of Reelin itself, which has been implicated in regulating granule cell migration (Frotscher et al., 2003; Sibbe et al., 2009), contribute to delayed establishment of the SPZ in *Nestin*-Cre;*Tbr2*$^{flox/flox}$ mice, particularly since we have shown that fewer Reelin + cells populate the hippocampal fissure at E16.5. However, others have reported that Reelin is not explicitly required for migration of progenitors to the SPZ, but rather that the *Cxcl12/Cxcr4* chemokine signaling pathway is key for formation of the SPZ (Li et al., 2009). Interestingly, we show that this pathway is also disrupted in the DG of mutant mice, and that *Nestin*-Cre;*Tbr2*$^{flox/flox}$ mice share many similarities with *Cxcr4* knockout mice. Indeed, in *Cxcr4* knockout mice, formation of the transhilar radial glial scaffold is abnormal, with reduced Gfap+ processes present in the hilus (Bagri et al., 2002; Li et al., 2009). As well, Blbp+ cells fail to localize to the hilus and hippocampal fissure in *Cxcr4* null mice, and instead remain in the FDJ as we observed in *Nestin*-Cre;*Tbr2*$^{flox/flox}$ mice (Li et al., 2009). These findings suggest that downregulation of *Cxcr4* after *Tbr2* ablation likely impairs migration to the forming DG. Interestingly, during early DG development, *Cxcl12*

expression from the meninges is thought to regulate positioning of Cajal-Retzius cells in the dentate marginal zone (Paredes et al., 2006), suggesting that these two signaling pathways may work in concert to control early events in DG morphogenesis. Thus, the phenotype we describe in *Nestin*-Cre;*Tbr2*$^{flox/flox}$ mice may be the product of defective interplay between the Reelin and chemokine signaling pathways.

In addition to aberrant glial scaffold development, *Cxcr4* null mutants also exhibit an early burst of neurogenesis in the DMS that accompanies delayed migration of progenitors to the SPZ (Li et al., 2009), similar to *Nestin*-Cre;*Tbr2*$^{flox/flox}$ mice. Previous reports suggest that normal migration of NSCs/INPs to the DG and proper timing of differentiation are intrinsically coupled during early stages of DG development, with delayed progenitor migration resulting in early neuroblast generation in the DMS (Li et al., 2009). Coupling of migration and differentiation has also been shown in the postnatal rostral migratory stream, where delayed transit to the olfactory bulb alters the fate and physiological functions of newborn neuroblasts (Belvindrah et al., 2011). We suggest that delayed transit of progenitors to the SPZ contributes to the burst of premature neuroblast generation we observe in *Nestin*-Cre;*Tbr2*$^{flox/flox}$ mice. Interestingly, we noted premature neurogenesis only in embryonic *Nestin*-Cre;*Tbr2*$^{flox/flox}$ mice, suggesting that this phenomenon might be intrinsically coupled to the pace and timing of migration during early development when extensive migration of progenitors to the DG is underway. In fact, we showed previously that granule neurons are reduced in postnatal *Nestin*-Cre;*Tbr2*$^{flox/flox}$ mice as a result of failed differentiation of NSCs and accumulation of Sox2+ NSCs in the DG (Hodge et al., 2012). In addition, we previously established that *Tbr2* likely represses *Sox2* during the transition from NSCs to INPs in the DG (Hodge et al., 2012). This may provide an explanation for why we observed aberrant co-expression of Sox2 and Prox1 in *Nestin*-Cre;*Tbr2*$^{flox/flox}$ mice. Perhaps, in the absence of *Tbr2*, *Sox2* is not repressed during differentiation, resulting in the unusual coexpression of Sox2 and Prox1 that we noted in the DMS of mutant mice. In any case, these perturbations clearly result in a cellular phenotype that is incompatible with cell survival and, accordingly, we observed a substantial increase in cell death in the DG of *Nestin*-Cre;*Tbr2*$^{flox/flox}$ mice.

The existence of the SPZ and its role as a transient neurogenic niche that contributes to the generation of granule neurons and establishment of the SGZ has only been recognized recently (Li et al., 2009). We show here that several steps in the development of the SPZ are impacted by loss of *Tbr2* expression. Firstly, initial formation of the SPZ is affected in *Nestin*-Cre;*Tbr2*$^{flox/flox}$ mice, perhaps as a result of a *Cxcr4/Cxcl12* and/or Reelin dependent defect in migration of progenitors as discussed above. Additionally, our results indicate that NSCs fail to exit the SPZ in a timely fashion to contribute to the SGZ, and instead accumulate in the SPZ of mutant mice. Previous studies have shown that Reelin expression regulates exit of progenitor cells from the SPZ (Li et al., 2009). Thus, it is possible that the decreased number of Cajal-Retzius cells present in the *Nestin*-Cre;*Tbr2*$^{flox/flox}$ hippocampal fissure results in a large enough reduction in available Reelin to influence the exit of progenitors from the SPZ. Further studies will be required to determine the exact mechanisms responsible for regulating the dynamics of SPZ progenitors and their transition from the SPZ to SGZ in order to fully understand the failure of these cells to exit the SPZ in *Nestin*-Cre;*Tbr2*$^{flox/flox}$ mice. In any case, our results indicate that *Tbr2* is critically important for the development of this transient niche and for subsequent establishment of the SGZ, further highlighting the requirement for *Tbr2* during DG morphogenesis.

Acknowledgments

Project support was from NIMH 3R01- MH080766 and R01-MH058869 to RFH. RDH received fellowships from the Heart & Stroke Foundation of Canada and the American Heart Association (10POST2610067). Roderick Yang

provided technical assistance. S.J. Pleasure (University of California, San Francisco) provided the Prox1 antibody as well as *Cxcr4* and *Cxcl12* plasmids, and E. Grove (University of Chicago) kindly provided plasmids for *Wnt3a* and *Wnt5a*. Nestin-GFP mice were from G. Enikolopov (Cold Spring Harbor Labs), and *Nestin*-CreER^{T2} mice were generously provided by R. Kageyama (Kyoto University).

References

Arnold SJ, Huang G-J, Cheung AFP, Era T, Nishikawa S-I, Bikoff EK, Molnar Z, Robertson EJ, Groszer M. The T-box transcription factor Eomes/Tbr2 regulates neurogenesis in the cortical subventricular zone. Genes Dev. 2008; 22:2479–2484. [PubMed: 18794345]

Bagri A, Gurney T, He X, Zou YR, Littman DR, Tessier-Lavigne M, Pleasure SJ. The chemokine SDF1 regulates migration of dentate granule cells. Development. 2002; 129:4249–4260. [PubMed: 12183377]

Bedogni F, Hodge RD, Elsen GE, Nelson BR, Daza RAM, Beyer RP, Bammler TK, Rubenstein JLR, Hevner RF. Tbr1 regulates regional and laminar identity of postmitotic neurons in developing neocortex. Proc Natl Acad Sci USA. 2010; 107:13129–13134. [PubMed: 20615956]

Belvindrah R, Nissant A, Lledo PM. Abnormal neuronal migration changes the fate of developing neurons in the postnatal olfactory bulb. J Neurosci. 2011; 31:7551–7562. [PubMed: 21593340]

Berger O, Li G, Han SM, Paredes M, Pleasure SJ. Expression of SDF-1 and CXCR4 during reorganization of the postnatal dentate gyrus. Dev Neurosci. 2007; 29:48–58. [PubMed: 17148948]

Englund C, Fink A, Lau C, Pham D, Daza RAM, Bulfone A, Kowalczyk T, Hevner RF. Pax6, Tbr2, and Tbr1 are expressed sequentially by radial glia, intermediate progenitor cells, and postmitotic neurons in developing neocortex. J Neurosci. 2005; 25:247–251. [PubMed: 15634788]

Forster E, Tielsch A, Saum B, Weiss KH, Johanssen C, Graus-Porta D, Muller U, Frotscher M. Reelin, Disabled 1, and beta 1 integrins are required for the formation of the radial glial scaffold in the hippocampus. Proc Natl Acad Sci USA. 2002; 99:13178–13183. [PubMed: 12244214]

Frotscher M, Haas CA, Forster E. Reelin controls granule cell migration in the dentate gyrus by acting on the radial glial scaffold. Cereb Cortex. 2003; 13:634–640. [PubMed: 12764039]

Grove EA, Tole S, Limon J, Yip L, Ragsdale CW. The hem of the cerebral cortex is defined by the expression of multiple Wnt genes and is compromised in Gli3-deficient mice. Development. 1998; 125:2315–2325. [PubMed: 9584130]

Gu X, Liu B, Wu X, Yan Y, Zhang Y, Wei Y, Pleasure SJ, Zhao C. Inducible genetic lineage tracing of cortical hem derived Cajal-Retzius cells reveals novel properties. PLoS ONE. 2011; 6:e28653. [PubMed: 22174859]

Hevner RF, Hodge RD, Daza RAM, Englund C. Transcription factors in glutamatergic neurogenesis: conserved programs in neocortex, cerebellum, and adult hippocampus. Neurosci Res. 2006; 55:223–233. [PubMed: 16621079]

Hodge RD, D'Ercole AJ, O'Kusky JR. Increased expression of insulin-like growth factor-I (IGF-I) during embryonic development produces neocortical overgrowth with differentially greater effects on specific cytoarchitectonic areas and cortical layers. Brain Res Dev Brain Res. 2005; 154:227–237.

Hodge RD, Nelson BR, Kahoud RJ, Yang R, Mussar KE, Reiner SL, Hevner RF. Tbr2 is essential for hippocampal lineage progression from neural stem cells to intermediate progenitors and neurons. J Neurosci. 2012; 32:6275–6287. [PubMed: 22553033]

Hodge RD, Kowalczyk TD, Wolf SA, Encinas JM, Rippey C, Enikolopov G, Kempermann G, Hevner RF. Intermediate progenitors in adult hippocampal neurogenesis: Tbr2 expression and coordinate regulation of neuronal output. J Neurosci. 2008; 28:3707–3717. [PubMed: 18385329]

Imayoshi I, Ohtsuka T, Metzger D, Chambon P, Kageyama R. Temporal regulation of Cre recombinase activity in neural stem cells. Genesis. 2006; 44:233–238. [PubMed: 16652364]

Intlekofer AM, Banerjee A, Takemoto N, Gordon SM, Dejong CS, Shin H, Hunter CA, Wherry EJ, Lindsten T, Reiner SL. Anomalous type 17 response to viral infection by CD8+ T cells lacking T-bet and eomesodermin. Science. 2008; 321:408–411. [PubMed: 18635804]

Lavado A, Oliver G. Prox1 expression patterns in the developing and adult murine brain. Dev Dyn. 2007; 236:518–524. [PubMed: 17117441]

Li G, Pleasure SJ. Morphogenesis of the dentate gyrus: what we are learning from mouse mutants. Dev Neurosci. 2005; 27:93–99. [PubMed: 16046842]

Li G, Kataoka H, Coughlin SR, Pleasure SJ. Identification of a transient subpial neurogenic zone in the developing dentate gyrus and its regulation by Cxcl12 and Reelin signaling. Development. 2009; 136:327–335. [PubMed: 19103804]

Liu M, Pleasure SJ, Collins AE, Neobels JL, Naya FJ, Tsai MJ, Lowenstein DH. Loss of BETA2/NeuroD leads to malformation of the dentate gyrus and epilepsy. Proc Natl Acad Sci USA. 2000; 97:865–870. [PubMed: 10639171]

Mignone JL, Kukekov V, Chiang A-S, Steindler D, Enikolopov G. Neural stem and progenitor cells in nestin-GFP transgenic mice. J Comp Neurol. 2004; 469:311–324. [PubMed: 14730584]

Mongiat LA, Esposito MS, Lombardi G, Schinder AF. Reliable activation of immature neurons in the adult hippocampus. PLoS ONE. 2009; 4:e5320. [PubMed: 19399173]

Paredes MF, Li G, Berger O, Baraban SC, Pleasure SJ. Stromal-derived factor-1 (CXCL12) regulates laminar position of Cajal-Retzius cells in normal and dysplastic brains. J Neurosci. 2006; 26:9404–9412. [PubMed: 16971524]

Pleasure SJ, Collins AE, Lowenstein DH. Unique expression patterns of cell fate molecules delineate sequential stages of dentate gyrus development. J Neurosci. 2000; 20:6095–6105. [PubMed: 10934259]

Roybon L, Hjalt T, Stott S, Guillemot F, Li J-Y, Brundin P, Reh TA. Neurogenin2 Directs Granule Neuroblast Production and Amplification while NeuroD1 Specifies Neuronal Fate during Hippocampal Neurogenesis. PLoS ONE. 2009; 4:e4779. [PubMed: 19274100]

Schwab MH, Batholomae A, Heimrich B, Feldmeyer D, Druffel-Augustin S, Goebbels S, Naya FJ, Zhao S, Frotscher M, Tsai MJ, Nave KA. Neuronal basic helix-loop-helix proteins (NEX and BETA2/NeuroD) regulate termina granule cell differentiation in the hippocampus. J Neurosci. 2000; 20:3714–3724. [PubMed: 10804213]

Shimogori T, Banuchi V, Ng HY, Strauss JB, Grove EA. Embryonic signalling centers expressing BMP, Wnt, and FGF proteins interact to pattern the cerebral cortex. Development. 2004; 131:5639–5647. [PubMed: 15509764]

Sibbe M, Forster E, Basak O, Taylor V, Frotscher M. Reelin and Notch1 Cooperate in the Development of the Dentate Gyrus. J Neurosci. 2009; 29:8578–8585. [PubMed: 19571148]

Toni N, Laplagne DA, Zhao C, Lombardi G, Ribak CE, Gage FH, Schinder AF. Neurons born in the adult dentate gyrus form functional synapses with target cells. Nat Neurosci. 2008; 11:901–907. [PubMed: 18622400]

Tronche F, Kellendonk C, Kretz O, Gass P, Anlag K, Orban PC, Bock R, Klein R, Schutz G. Disruption of the glucocorticoid receptor gene in the nervous system results in reduced anxiety. Nat Genet. 1999; 23:99–103. [PubMed: 10471508]

Weiss KH, Johanssen C, Tielsch A, Herz J, Deller T, Frotscher M, Forster E. Malformation of the radial glial scaffold in the dentate gyrus of reeler mice, scrambler mice, and ApoER2/VLDLR-deficient mice. J Comp Neurol. 2003; 460:56–65. [PubMed: 12687696]

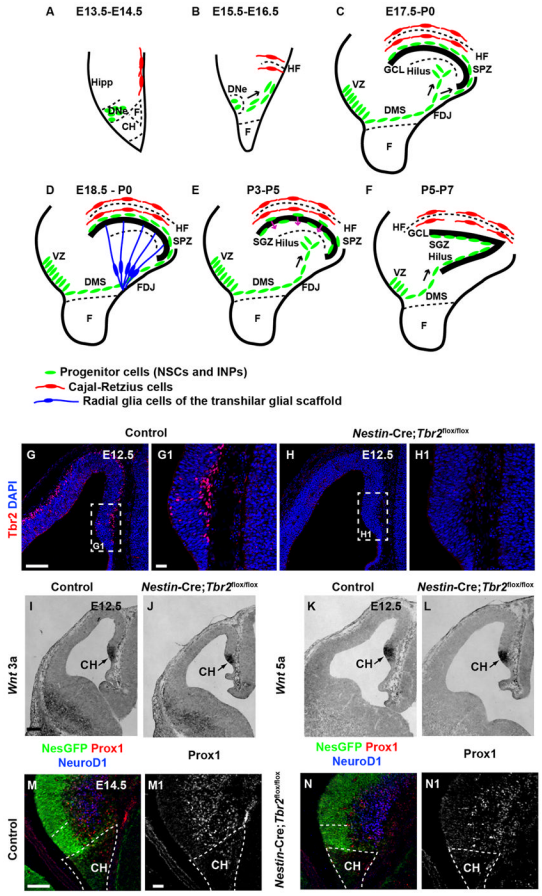

Figure 1. Early development of the DG is essentially normal in *Nestin*-Cre;*Tbr2*$^{flox/flox}$ mice

(A–F) Schematic diagram illustrating the steps in DG development. Progenitor cells (NSCs and INPS) are shown in green. Cajal-Retzius cells are shown in red. The transhilar radial glial scaffold is shown in blue. (A–B) Progenitor cells initially located in the dentate neuroepithelium (DNe) migrate to the primordial DG concurrent with invagination of the pial surface and migration of Cajal-Retzius cells to the hippocampal fissure (HF) between E13.5 and E16.5. (C) Continued migration of progenitors through the dentate migratory stream (DMS) contributes to formation of the subpial neurogenic zone (SPZ) during later stages of development (E17.5-P0). (D) The transhilar radial scaffold forms at approximately the same time as radial glia become localized to the fimbriodentate junction (FDJ). (E) Transition of progenitor cells out of the SPZ occurs between P3–P5. (F) The subgranular zone (SGZ) neurogenic niche is established by P5–P7. (G-G1) Tbr2 protein (red) is expressed in cells in the cortical hem (CH) at E12.5 in control mice. (H-H1) Tbr2 protein is ablated in the cortical hem of mutant mice by E12.5. White dashed boxes in G and H represent areas shown at higher magnification in G1 and H1, respectively. (I–L) Expression of *Wnt3a* and *Wnt5a*, markers of the cortical hem, are present at approximately normal levels in *Nestin*-Cre;*Tbr2*$^{flox/flox}$ mice. (M–N, M1-N1) Markers of DG granule neurons (NeuroD1, Prox1) are present in the primordial DG of mutant mice, but are slightly reduced in comparison to controls as early as E14.5. Scale bars: G = 100 μm, G1 = 20 μm, I = 100 μm, M = 75 μm, M1 = 15 μm.

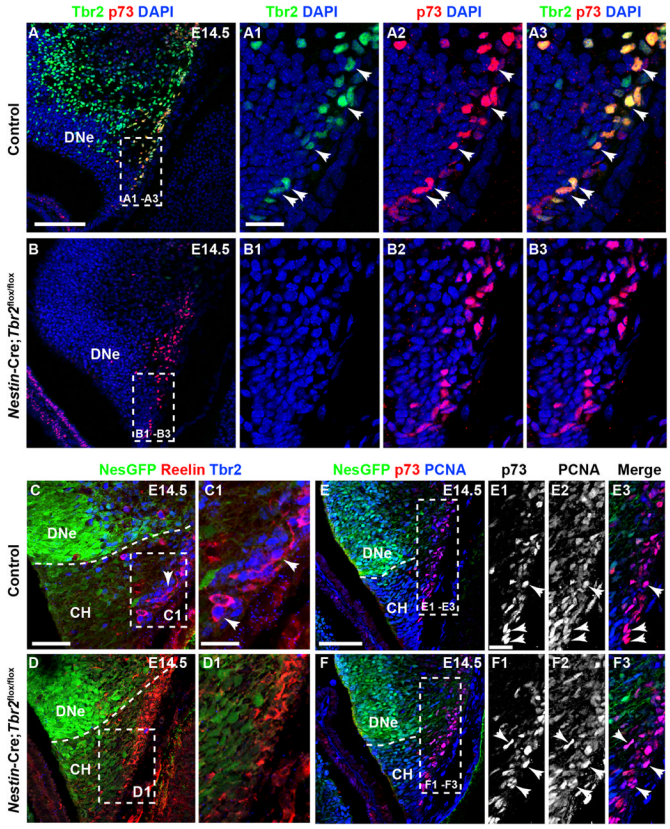

Figure 2. *Tbr2* expression is ablated in cortical hem-derived Cajal-Retzius cells in *Nestin*-Cre;*Tbr2*$^{flox/flox}$ mice

(A-A3) At E14.5 the majority of p73+ Cajal-Retzius cells in the cortical hem (CH) coexpress Tbr2 (arrows). (B-B3) p73 expression is maintained in the CH of *Nestin*-Cre;*Tbr2*$^{flox/flox}$ mice at E14.5; however, Tbr2 protein is absent from these cells (B2, B3). (C-D1) Similarly, Tbr2+ cells coexpress Reelin in the CH of control mice at E14.5, whereas Tbr2 protein is absent from Reelin+ Cajal-Retzius cells in *Nestin*-Cre;*Tbr2*$^{flox/flox}$ mice (D1). Regardless, the density of Cajal-Retzius cells in the CH of *Nestin*-Cre;*Tbr2*$^{flox/flox}$ mice appears approximately equivalent to controls at E14.5, as evidenced by Reelin (D1) and p73 staining (B3). (E-F3) Likewise, proliferation of Cajal-Retzius cells in the CH appears unaffected by ablation of Tbr2, as an approximately equivalent number of p73+ cells coexpress PCNA (arrows) in controls (E1–E3) and *Nestin*-Cre;*Tbr2*$^{flox/flox}$ mice (F1–F3). Scale bars: A = 150 μm, A1 = 50 μm, C = 100 μm, C1 = 30 μm, E = 100 μm, E1 = 15 μm. Regions delineated by dashed white boxes are shown in higher magnification in their respective adjacent panels.

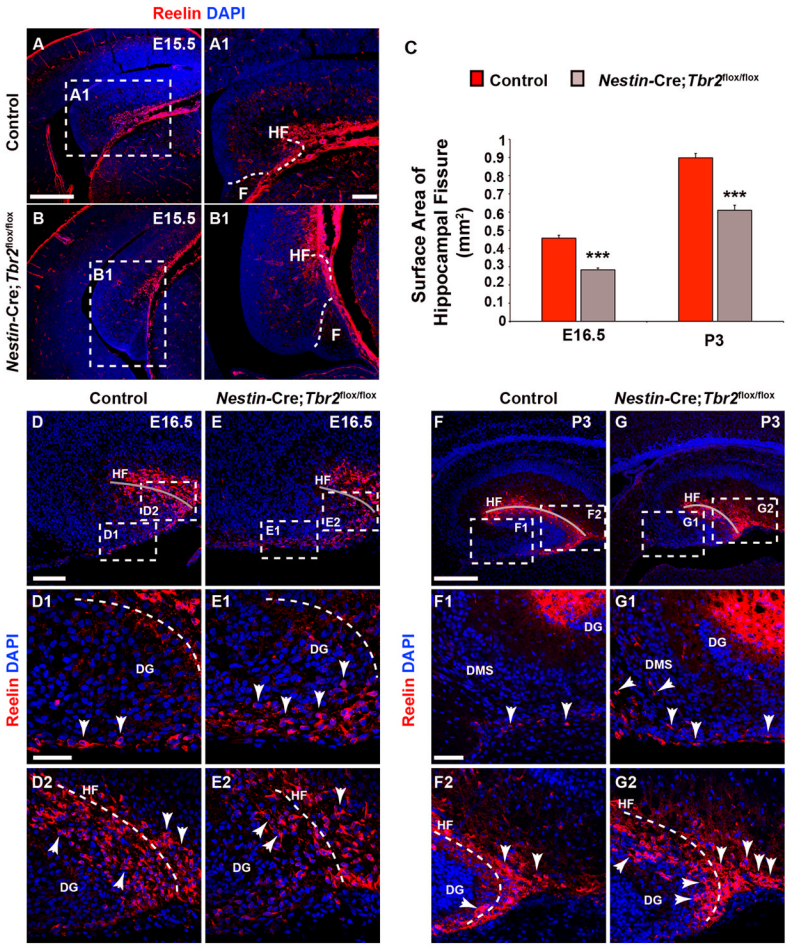

Figure 3. Rotation of the hippocampus and formation of the hippocampal fissure are abnormal in *Nestin*-Cre;*Tbr2*$^{flox/flox}$ mice

(A-A1) In control mice, invagination of the pial surface to form the hippocampal fissure (HF) occurs concurrent with rotation of the developing hippocampus. (B-B1) In *Nestin*-Cre;*Tbr2*$^{flox/flox}$ mice, rotation of the hippocampus is impaired, such that the DG appears to be rotated 90° in mutant mice in comparison to controls (compare A and B). (B-B1) As well, invagination of the pial surface is delayed in mutant mice, resulting in a reduction in the size of the HF. (C) Consistent with delayed invagination of the pial surface in *Nestin*-Cre;*Tbr2*$^{flox/flox}$ mice, the surface area of the HF is persistently and significantly reduced in mutant mice (ANOVA, N=3, P<0.001). Graphs in (C) represent the mean ±SEM (**P<0.01, ***P<0.001). (D-D2) By E16.5, the majority of Reelin+ Cajal-Retzius cells are localized to the HF (grey line) in control mice (D2), and a smaller population of these cells can be seen in the dentate migratory stream (DMS). (E-E2) In contrast, the DMS is rich in Reelin+ Cajal-Retzius cells in *Nestin*-Cre;*Tbr2*$^{flox/flox}$ mice and there are fewer of these cells located in the HF in mutant mice, suggesting impaired migration and ectopic localization of these cells in mutants. The reduction in HF surface area is also evident in mutant mice (compare grey lines in D, E and compare D2 and E2). (F-F2) By P3, very few Reelin+ Cajal-Retzius cells remain in the DMS in control mice (arrows), and the bulk of these cells are located in the HF (F2), which has increased in surface area with continued growth of the DG in comparison to controls at E16.5. (G-G2) However, in *Nestin*-Cre;*Tbr2*$^{flox/flox}$ mice ectopic Reelin+ cells can been seen in the DMS (G1, arrows) at P3, suggesting impaired migration of these cells to the HF. (G2) In mutant mice, there is also an increased concentration of

Reelin+ cells at the tip of the DG arrows in comparison to controls (F, F2), further supporting ectopic localization of Cajal-Retzius cells in *Nestin*-Cre;*Tbr2*$^{flox/flox}$ mice. Scale bars: A = 200 μm, A1 = 50μm, D = 175 μm, D1 = 50 μm, F = 175 μm, F1 = 75 μm. Regions delineated by dashed white boxes are shown in higher magnification in their respective adjacent panels. Grey lines in D-G highlight the HF in each panel.

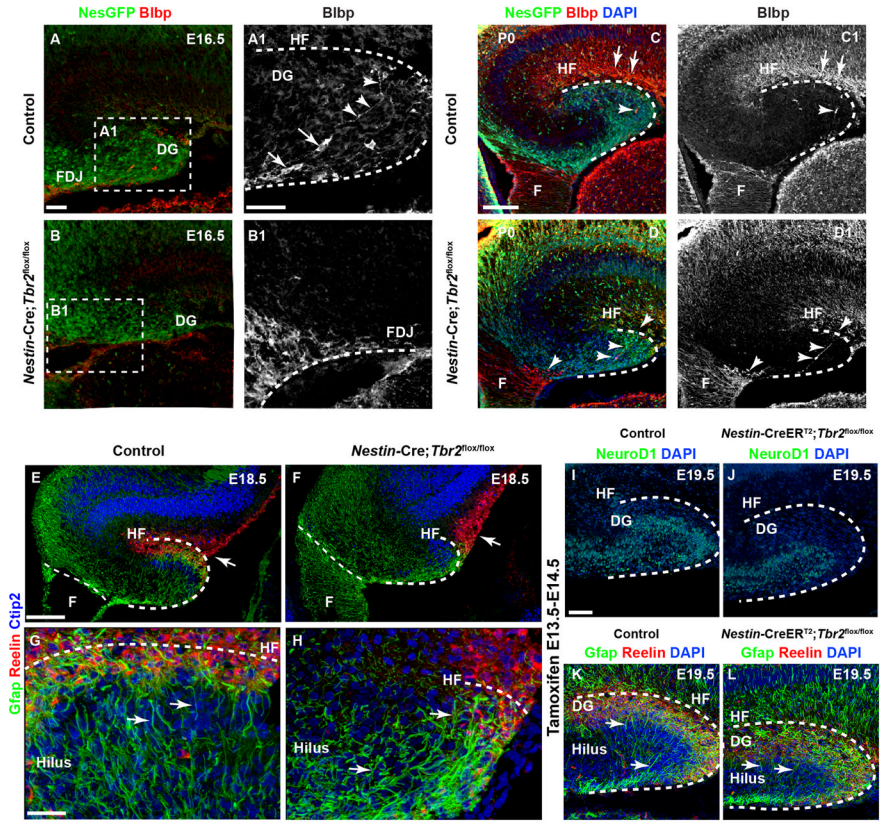

Figure 4. Development of the transhilar radial glial scaffold is perturbed after ablation of *Tbr2*.

(A-A1) In E16.5 control mice, Blbp+ radial glia exit the dentate ventricular zone and migrate to the hippocampal fissure (HF) to take up residence in the dentate marginal zone. They can be seen exiting the fimbriodentate junction (FDJ) region and migrating across the hilus (A1, cell bodies are marked by arrows and associated processes by arrowheads). (B-B1) Migration of Blbp+ cells is delayed in *Nestin*-Cre;*Tbr2*$^{flox/flox}$ mice and accumulation of Blbp+ cells is apparent in the fimbria and FDJ. Regions delineated by dashed white boxes are shown in higher magnification in their respective adjacent panels (A1, B1). (C-C1) By P0, Blbp+ cell migration is essentially complete in control mice, and enrichment of Blbp+ processes is apparent in the HF. (D-D1, arrows) In *Nestin*-Cre;*Tbr2*$^{flox/flox}$ mice, Blbp+ cells remain concentrated in the fimbria and FDJ and only rarely can be seen migrating to the HF (arrowheads). (E–H) Gfap+ processes making up the transhilar glial scaffold are aberrant in *Nestin*-Cre;*Tbr2*$^{flox/flox}$ mice. In control mice (E, G) Gfap+ processes exhibit clear radial orientation across the hilus, whereas Gfap+ processes are oriented either randomly or towards the reduced HF where Reelin+ Cajal-Retzius cells are located in *Nestin*-Cre;*Tbr2*$^{flox/flox}$ mice (F, H, arrows). These processes do not exhibit the clear radial orientation typically seen in control mice (G, H, arrows). (I–L) *Tbr2* ablation on E13.5-E14.5 rescues DG morphogenetic defects. Inducible conditional deletion of *Tbr2* (*Nestin*-CreER^{T2};*Tbr2*$^{flox/flox}$) was achieved by treating mice with tamoxifen on E13.5 and E14.5. Control mice were *Nestin*-CreER^{T2};*Tbr2*$^{flox/+}$. (I–J) Consistent with the known role of *Tbr2* in regulating granule cell neurogenesis, NeuroD1+ neuroblasts are reduced in the developing DG of *Nestin*-CreER^{T2};*Tbr2*$^{flox/flox}$ mice, resulting in a decrease in the overall size of the DG (J) at E19.5. However, the HF is approximately the same size in controls (K) and *Nestin*-CreER^{T2};*Tbr2*$^{flox/flox}$ mice (L). Reelin+ Cajal-Retzius cells are abundant in the dentate marginal zone adjacent to the HF in both controls (K) and *Nestin*-CreER^{T2};*Tbr2*$^{flox/flox}$ mice(L), and Gfap+ processes are radially oriented across the hilus in

both groups (K–L, arrows) consistent with normal development of the transhilar radial scaffold. Scale bars: A = 50 μm, A1 = 30 μm, C = 75 μm, E = 100 μm, G = 30 μm, I = 50 μm.

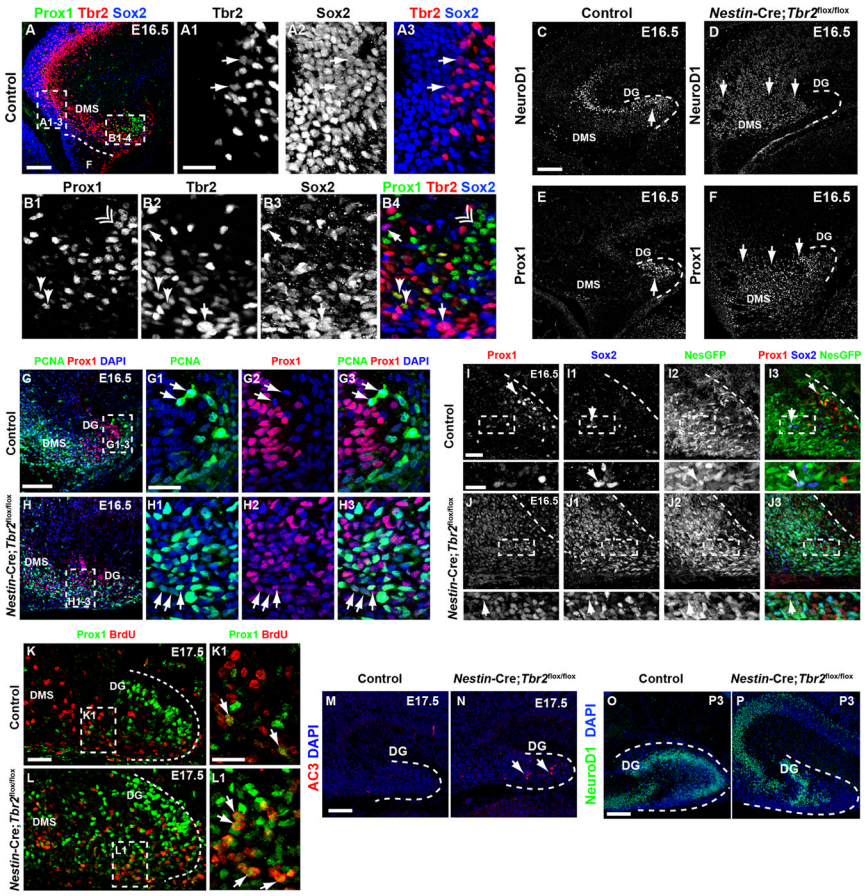

Figure 5. Premature granule cell neurogenesis is apparent in *Nestin*-Cre;*Tbr2*$^{flox/flox}$ mice

(A-A3) In control mice, Sox2 and Tbr2 are coexpressed in a subset of cells (A1-A3, arrows) in the dentate ventricular zone, whereas Prox1 is not expressed in this region but rather is restricted to the dentate migratory stream (DMS) and developing DG (A). However, Sox2+/Tbr2+ cells represent a relatively minor fraction of the total Sox2+ population, consistent with the notion that Sox2 is predominantly expressed in NSCs, whereas Tbr2 is largely restricted to INPs (A1–A3). (B1–B4) Within the DMS, Tbr2 and Sox2 continue to be coexpressed in a subset of cells, and these cells are Prox1-negative (B1–B4, arrows). However, coexpression of Tbr2 and Prox1 is apparent in a small subset of Tbr2+ cells, but these Tbr2+/Prox1+ cells are Sox2-negative (B1–B4, arrowheads). Prox1 and Sox2 coexpression is very rare in control animals at E16.5, consistent with downregulation of Sox2 during neuronal differentiation. Accordingly, most Prox1+ cells do not coexpress Sox2 or Tbr2 (double arrowhead, B1–B4). (C) In control mice, NeuroD1+ neuroblasts are present in the forming suprapyramidal blade of the DG (arrow) and in the hippocampal CA3 field. Only scattered NeuroD1+ cells are present in the DMS in controls (C). (D) In *Nestin*-Cre;*Tbr2*$^{flox/flox}$ mice, numerous NeuroD1+ cells are present in the DMS, which appears to be expanded in comparison to controls, but relatively few are in the DG itself. (E) Prox1 protein is also mostly restricted to the forming DG in control mice, whereas Prox1 is expressed extensively in the expanded DMS of *Nestin*-Cre;*Tbr2*$^{flox/flox}$ mice, indicative of an early burst of neurogenesis in mutant animals at E16.5 (F). (G-G3) In control mice, Prox1+ neuroblasts rarely proliferate as evidenced by the scarcity of Prox1+/PCNA+ cells in these mice. Arrows in G1–G3 illustrate proliferating progenitors (PCNA+) that lack Prox1 expression in a control animal at E16.5 However, in *Nestin*-Cre;*Tbr2*$^{flox/flox}$ mice at E16.5, the number of proliferating (PCNA+) Prox1+ neuroblasts is increased (arrows H1–H3)

within the expanded DMS and developing DG. Although, PCNA+/Prox1+ cells appear to express Prox1 at low levels and these cells still represent a minority of the total population of Prox1+ neuroblasts in mutant mice (H1–H3). (I-I3) In control mice at E16.5, Prox1+ neuroblasts very rarely coexpress the NSC markers Sox2 and Nestin-GFP (NesGFP), consistent with downregulation of these NSC markers in neuroblasts. (J-J3) Conversely, in *Nestin*-Cre;*Tbr2*$^{flox/flox}$ mice there is extensive, unusual colocalization of Prox1, Sox2, and Nestin-GFP in the DG. Similar to our observations of Prox1+/PCNA+ cells in mutant mice (H1-H3), Prox1 appears to be expressed at low levels in these mutant Prox1+/Sox2+/NesGFP+ cells (J-J3). (K-L1) BrdU pulse-chase labeling (BrdU injected on E15.5. with embryo collection on E17.5) shows that the percentage of Prox1+/BrdU+ cells is increased in *Nestin*-Cre;*Tbr2*$^{flox/flox}$ mice (L-L1, arrows) in comparison to controls (K-K1, arrows), confirming premature neurogenesis in mutant mice during embryonic DG development. (M–N) The density of Activated-Caspase 3+ cells (AC3) is increased in *Nestin*-Cre;*Tbr2*$^{flox/flox}$ mice indicating that cell death is increased during this period of premature neurogenesis in mutants (N, arrows). (O–P) By P3, the suprapyramidal blade of the DG is easily identifiable in control mice and contains numerous NeuroD1+ neuroblasts, whereas these cells are reduced and misplaced in *Nestin*-Cre;*Tbr2*$^{flox/flox}$ mice. Scale bars: A = 100 μm, A1 = 50 μm, C = 100 μm, G = 100 μm, G1 = 35 μm, I = 35 μm, I (inset) = 20 μm, K = 100 μm, K1 35 μm, M = 75 μm, O = 75 μm. Regions delineated by dashed white boxes are shown in higher magnification in their respective adjacent panels.

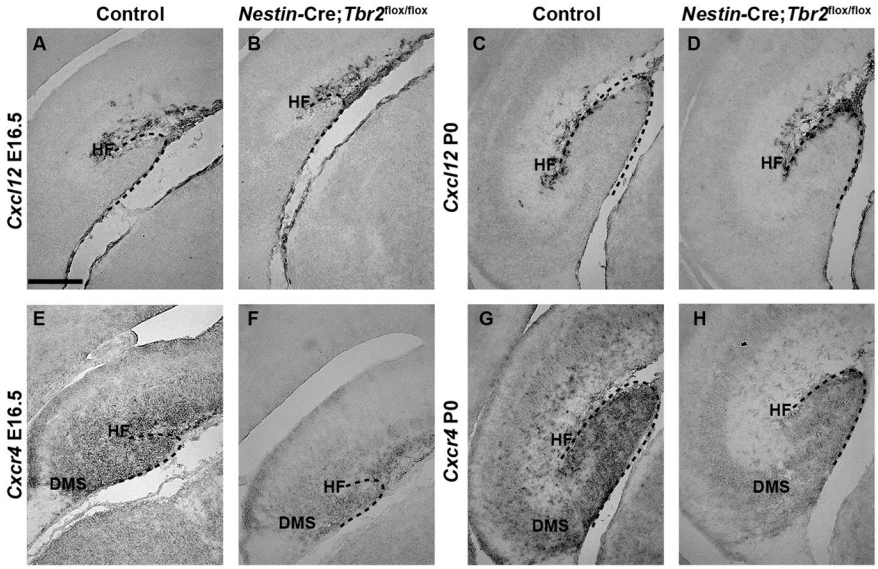

Figure 6. *Cxcr4* is downregulated in the DG of *Nestin*-Cre;*Tbr2*$^{flox/flox}$ mice

(A–D) *Cxcl12* expression is apparent in the meninges in the hippocampal fissure (HF) in both control and *Nestin*-Cre;*Tbr2*$^{flox/flox}$ mice at E16.5 and P0. Expression of *Cxcl12* on a per cell basis appears normal in *Nestin*-Cre;*Tbr2*$^{flox/flox}$ mice at both ages, although reduction of the HF and decreased numbers of *Cxcl12* expressing cells in the HF are readily apparent in mutants. (E–H) *Cxcr4*, the receptor for *Cxcl12* that is expressed on migrating progenitors and neuroblasts, is downregulated in the DG of *Nestin*-Cre;*Tbr2*$^{flox/flox}$ mice in comparison to controls at both E16.5 and P0. Scale bar: A = 100 μm.

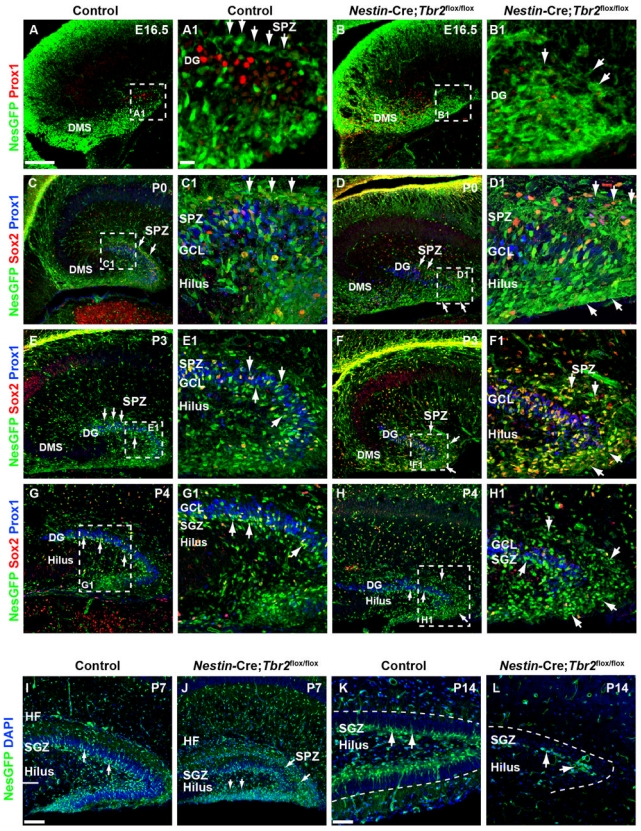

Figure 7. Development of the SGZ neurogenic niche is disrupted in *Nestin*- Cre;*Tbr2*$^{flox/flox}$ mice

(A-A1) The SPZ is apparent in controls by E16.5 as a layer of Nestin- GFP+ (NesGFP) cells immediately above the Prox1+ neuroblasts populating the forming upper DG blade (A1, arrows). (B-B1) In *Nestin*-Cre;*Tbr2*$^{flox/flox}$ mice, there is a delay in the formation of the SPZ (B1, arrows). In controls, NesGFP+ NSCs localize to the subpial neurogenic zone (SPZ) above the forming suprapyramidal blade on P0 (C-C1, arrows). In *Nestin*-Cre;*Tbr2*$^{flox/flox}$ mice, increased numbers of NesGFP+/Sox2+ cells are apparent in the SPZ on P0 (D-D1, arrows). By P3, NesGFP+ progenitors begin to transition out of the SPZ in control mice (E-E1, arrows). In contrast, many NesGFP+ NSCs remain concentrated in the SPZ in *Nestin*-Cre;*Tbr2*$^{flox/flox}$ mice, although some do migrate through the GCL (F-F1). By P4, transition of NSCs out of the SPZ is largely complete in control mice and the SGZ is apparent adjacent to the hilus (G-G1, arrows). In mutant mice on P4, NesGFP+ NSCs remain concentrated in the SPZ and are reduced in the SGZ (H-H1, arrows). In controls NesGFP+ NSCs are apparent in the SGZ and the transitory SPZ is essentially gone by P7 (I). At P7, Many NesGFP+ NSCs remain in the SPZ in *Nestin*-Cre;*Tbr2*$^{flox/flox}$ mice (J, arrows) and are also present in the hilus. By P14, NesGFP+ progenitor cells are exclusively found in the SGZ in control mice (K). In *Nestin*-Cre;*Tbr2*$^{flox/flox}$ mice, the SGZ is present, but is reduced in size (L) with very few NesGFP+ NSCs present. Scale bars: A = 100 μm, A1 = 25 μm, I = 75 μm, K = 30 μm. Regions delineated by dashed white boxes are shown in higher magnification in their respective adjacent panels.

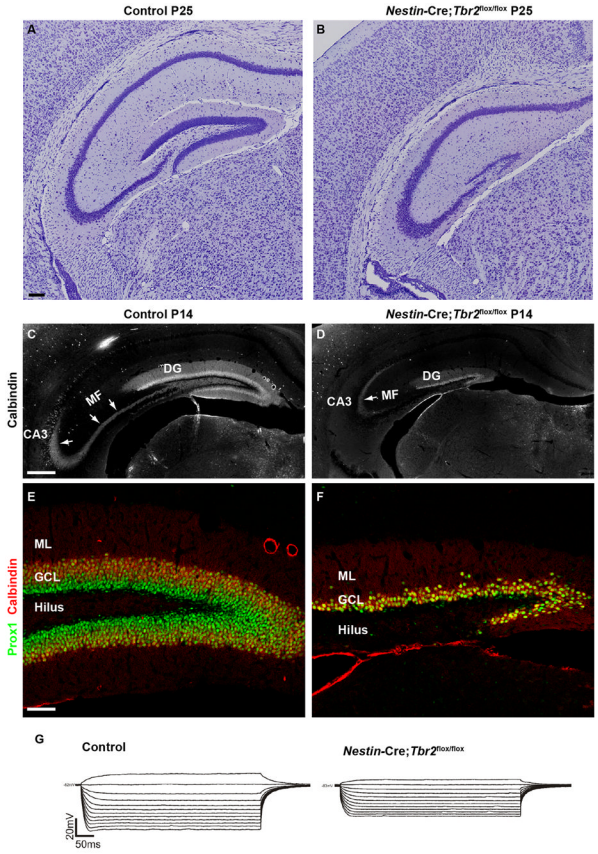

Figure 8. *Tbr2* ablation has severe consequences for DG morphogenesis

(A–B) By early postnatal development, the DG of control mice is fully formed, whereas the DG of *Nestin*-Cre;*Tbr2*$^{flox/flox}$ mice consists only of a truncated and thinned suprapyramidal blade. (B) The infrapyramidal blade of the GCL essentially fails to form in *Nestin*-Cre;*Tbr2*$^{flox/flox}$ mice. (C) The mossy fiber pathway (MF), the main output of the DG granule neurons to CA3 is easily distinguished by immunostaining for Calbindin at P14 in control animals (C, arrows). (D) In mutant mice the MF pathway is greatly reduced (D, arrow) owing to the decrease in DG size. (E–F) The cells that remain in the DG of *Nestin*-Cre;*Tbr2*$^{flox/flox}$ mice appear to be granule neurons as evidenced by their expression of Prox1 and Calbindin. However, the number of granule neurons populating the DG is clearly greatly reduced in mutant mice (F) in comparison to controls (E). (G) Representative I-V curves from control and *Nestin*-Cre;*Tbr2*$^{flox/flox}$ mice illustrate that input resistance is significantly decreased in granule neurons remaining in the reduced DG of mutant mice in comparison to controls. Scale bars: A = 100 μm, C = 100μm, E = 100 μm.

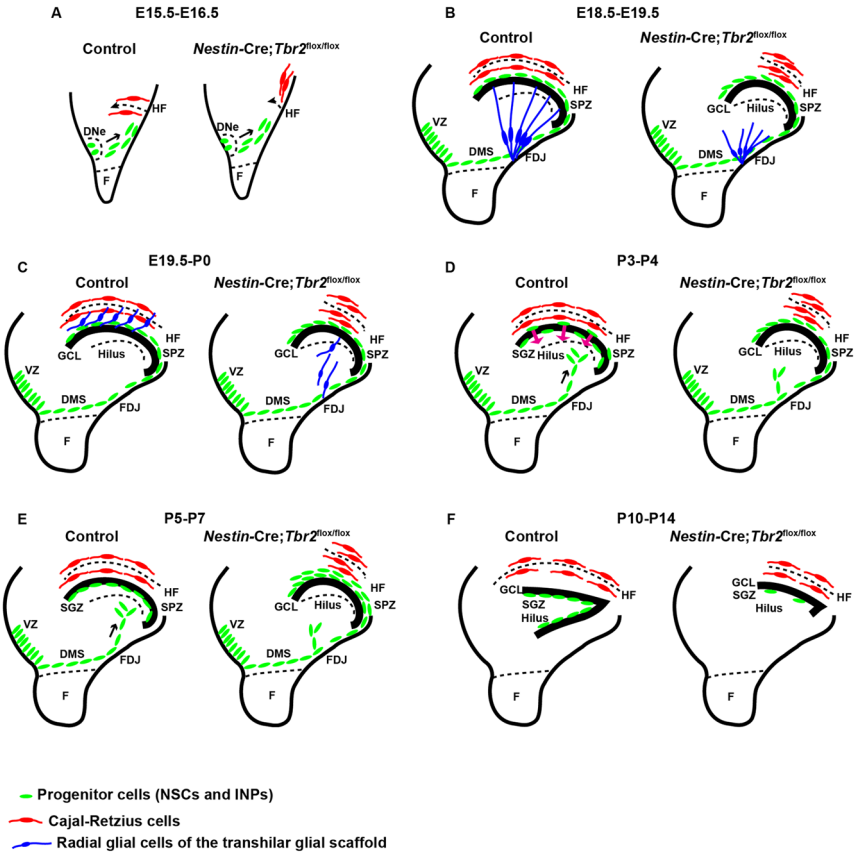

Figure 9. Schematic diagram summarizing DG defects in *Nestin*-Cre;*Tbr2*$^{flox/flox}$ mice

(A) Initial invagination of the pial surface is delayed in *Nestin*-Cre;*Tbr2*$^{flox/flox}$ mice, and the migration of Cajal-Retzius cells (red) to the forming hippocampal fissure (HF) is delayed in mutants. (B) Development of the transhilar radial glial scaffold (blue cells) is abnormal in *Nestin*-Cre;*Tbr2*$^{flox/flox}$ mice by E18.5–E19.5, and the number of Cajal-Retzius cells (red) populating the HF is reduced. (C) Blbp+ radial glial cells (blue) that contribute to the transhilar radial glial scaffold complete their redistribution to the HF by E19.5-P0 in control mice, but this migration is delayed in *Nestin*-Cre;*Tbr2*$^{flox/flox}$ mice. (D) During early postnatal development (P3–P4) progenitor cells (green) populating the transient SPZ are redistributed to form the SGZ niche. In *Nestin*-Cre;*Tbr2*$^{flox/flox}$ mice, these cells are retained in the SPZ and fail to migrate to the SGZ. (E) Formation of the SGZ (green, progenitor cells) is complete by P5–P7 in control mice and the SPZ is no longer apparent. In mutant mice, retention of progenitors in the SPZ persists. (F) By P10–P14 both the suprapyramidal and infrapyramidal blades of the DG are formed in control mice, and progenitor cells (NSCs and INPS, green) are localized to the SGZ. In *Nestin*-Cre;*Tbr2*$^{flox/flox}$ mice, the infrapyramidal blade fails to form, the suprapyramidal blade is reduced in size, and progenitor cells are nearly absent from the SGZ (green).